

研究论文

六核(3,3,4,5)-连接 2-(4'-羧基苯基)咪唑-4,5-二羧酸金属有机配合物

喻聪聪¹ 徐余幸¹ 管全银² 赵国良^{1,2*}(浙江师范大学¹行知学院²化学与生命科学学院 金华 321004)

摘要 用缩合氧化反应,成功合成了一个新的咪唑羧酸配体 2-(4'-羧基苯基)咪唑-4,5-二羧酸(H₄CPhIDC)。在水热条件下以 H₄CPhIDC 为主配体,邻菲咯啉(phen)为辅助配体,合成了镉的六核金属有机配合物[Cd₆(CPhIDC)(HCPhIDC)₂(H₂CPhIDC)(phen)₆]·H₂O (MOF)。H₄CPhIDC 配体在该配合物中呈现出不同的去质子模式 H₂CPhIDC²⁻、HCPhIDC³⁻、CPhIDC⁴⁻,从而形成了一个新的六核(3,3,4,5)-连接拓扑结构。测定了配体和配合物的固体荧光光谱,并用溴化乙锭荧光探针测定了配体和配合物与 DNA 及 BSA 的作用,结果表明,配合物对生物大分子的作用更强些。CCDC: 969815。

关键词 镉金属有机配合物 2-(4'-羧基苯基)咪唑-4,5-二羧酸 荧光光谱 DNA BSA

A New Six-Core (3,3,4,5)-Connected Metal-Organic Framework Topology Connected by 2-(4'-Carboxyphenyl)-1*H*-imidazole-4,5-dicarboxylic Acid

Yu Congcong¹, Xu Yuxing¹, Guan Quanyin², Zhao Guoliang^{1,2*}(¹Xingzhi College; ²College of Chemistry and Life Science, Zhejiang Normal University, Jinhua 321004)

Abstract A novel imidazole carboxylic acid ligand, 2-(4'-carboxyphenyl)-1*H*-imidazole-4,5-dicarboxylic acid (H₄CPhIDC) was prepared by condensation and oxidation reactions, and its metal-organic framework (MOF) [Cd₆(CPhIDC)(HCPhIDC)₂(H₂CPhIDC)(phen)₆]·H₂O (phen=1,10-phenanthroline) was synthesized by solvothermal reaction. The H₄CPhIDC ligand presents different deprotonated motifs of H₂CPhIDC²⁻, HCPhIDC³⁻, and CPhIDC⁴⁻ in this MOF and thus to form a new six-core (3,3,4,5)-connected topology. Meanwhile, the fluorescence properties of the ligand and the MOF in the solid state were determined. DNA and BSA binding properties of the ligand and the MOF were investigated. The results showed that the complex has much stronger interaction with biological macromolecules than the ligand. CCDC: 969815.

Keywords Cd MOF, 2-(4'-Carboxyphenyl)-1*H*-imidazole-4,5-dicarboxylic acid, Photoluminescence, DNA, BSA

Metal-organic frameworks (MOFs) of *N*-hetero-cyclic carboxylates have been widely considered to be one of the most effective approaches to synthesize novel MOFs^[1], because multi-oxygen and nitrogen atoms of these building blocks can coordinate with metal ions in versatile ways, resulted in the formation of various MOFs with specific topologies^[2,3] and useful properties. As for imidazole carboxylic acids and imidazole derivatives, they have significant biological activities^[4]. Imidazole-4,5-dicarboxylic acid (H₃IDC), which can be partially or fully deprotonated to generate H₂IDC⁻, H₁IDC²⁻, and IDC³⁻ at different pH values and afford various coordination modes, is favored by multitudinous research groups. According to the reported MOFs^[5-12] constructed from H₃IDC, this ligand still remains extremely wide research area. Recently, purposefully changing the substituent group on the 2-position of imidazole-4,5-dicarboxylic acid has been an

喻聪聪 女, 22 岁, 本科生。*联系人, 赵国良 男, 教授, 主要从事功能配合物研究。E-mail: sky53@zjnu.cn

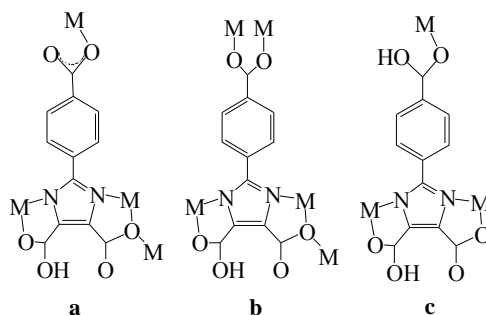
浙江省自然科学基金项目(LY12B01003)资助

2015-06-05 收稿, 2015-07-06 接受

effective way to obtain excellent ligands which can be used to construct MOFs with rapidly changing topological structures and useful properties, such as 2-methyl-1*H*-imidazole-4,5-dicarboxylic acid, 2-ethyl-1*H*-imidazole-4,5-dicarboxylic acid, 2-propyl-1*H*-imidazole-4,5-dicarboxylic acid, 2-phenyl-1*H*-imidazole-4,5-dicarboxylic acid, 2-hydroxymethyl-1*H*-imidazole-4,5-dicarboxylic acid and 2-(pyridyl)-1*H*-imidazole-4,5-dicarboxylic acid.

As the factors mentioned above, a new H₃IDC derivative 2-(4'-carboxyphenyl)-1*H*-imidazole-4,5-dicarboxylic acid (H₄CPhIDC)^[13] was purposely synthesized by condensation and oxidation reactions based on *o*-phenylenediamine and methyl 4-formylbenzoate. It is worthwhile to note that it's the first time to introduce carboxyl-containing group on the 2-position^[14] of H₃IDC and successfully applied to constructing MOF. The ligand H₄CPhIDC not only can be partially or fully deprotonated to H₃CPhIDC⁻, H₂CPhIDC²⁻, HCPhIDC³⁻ and CPhIDC⁴⁻, but also can exhibit very flexible coordination modes (Scheme 1), and hence may also result in a large diversity of supramolecular architectures.

We are interested in constructing MOFs with novel topology and interesting properties from the H₄CPhIDC and phen ligand. As expected, one unprecedented novel six-core MOF was synthesized by a solvothermal reaction.



Scheme 1 The coordination modes of the imidazole carboxylic acid anions for this MOF
图式 1 配合物中咪唑羧酸阴离子的配位模式

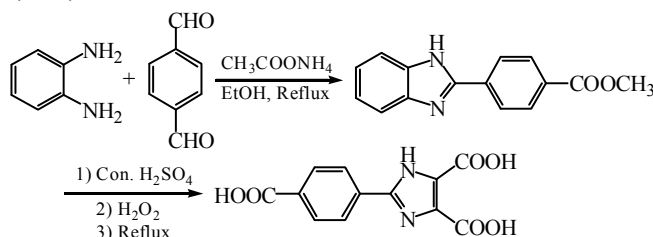
1 Experimental

1.1 Materials and measurements

All the reagents were of analytical grade and used without further purification. Elemental analysis was performed on C, H, N elemental analyzer, Elementar Vario EL III. FT-IR spectra were recorded on a Nicolet NEXUS 670 FTIR spectrophotometer using KBr discs in the range of 4000–400 cm⁻¹. Crystallographic data of the MOFs were collected on a Bruker Smart Apex II CCD diffractometer. Fluorescence spectra were measured at room temperature with an Edinburgh FL-FS920 TCSPC system.

1.2 Synthesis of 2-(4'-carboxyphenyl)-1*H*-imidazole-4,5-dicarboxylic acid^[14]

The ligand was synthesized according to literature^[14] (Scheme 2). ¹H NMR (400 MHz, DMSO-*d*₆) δ : 8.24 (s, 2H), 8.04 (d, *J* = 8.1 Hz, 2H); ¹³C NMR (101 MHz, DMSO-*d*₆) δ : 167.02, 161.32, 145.49, 133.35, 131.21, 130.05, 129.20, 128.47; Anal. calcd for C₁₂H₈O₆N₂(Mr = 276): C 52.17, H 2.90, N 10.15; found: C 52.10, H 2.85, N 10.10; IR(KBr) ν /cm⁻¹: 3435, 3011, 1942, 1716, 1555, 1413, 1265, 864, 716, 634.



Scheme 2 Preparation of 2-(4'-carboxyphenyl)-1*H*-imidazole-4,5-dicarboxylic acid.
图式 2 2-(4'-羧基苯基)咪唑-4,5-二羧酸的制备

1.3 Synthesis of $[\text{Cd}_6(\text{CPhIDC})(\text{HCPHIDC})_2(\text{H}_2\text{CPhIDC})(\text{phen})_6]\cdot\text{H}_2\text{O}$

A mixture of H_4CPhIDC (0.028 g, 0.1 mmol), phen (0.030 g, 0.15 mmol), $\text{Cd}(\text{OH})_2$ (0.022 g, 0.15 mmol) and H_2O (10 mL) was sealed in a 20 mL Teflon-lined stainless steel vessel and heated at 160 °C for 3 d. After the mixture being cooled to room temperature at a rate of 10 °C/h, colorless crystals suitable for single-crystal analysis and physical measurements were obtained, washed with distilled water, and dried in air. Yield: 30 % (based on H_4CPhIDC). Anal. Calcd. for $\text{C}_{120}\text{H}_{70}\text{N}_{20}\text{O}_{25}\text{Cd}_6$ (Mr = 2866.42): C 50.24, H 2.44, N 9.77; found: C 50.12, H 2.37, N 9.70; IR (KBr) ν/cm^{-1} : 3415, 1676, 1589, 1541, 1397, 1278, 1227, 1101, 979, 859, 793, 726, 638.

2 Results and Discussion

2.1 X-ray diffraction analysis

The single crystals of the MOF with approximate dimensions were mounted on a Bruker Smart Apex II CCD diffractometer. The diffraction data were collected using a graphite monochromated Mo K_α radiation ($\lambda = 0.71073 \text{ \AA}$) at 296(2) K. The employed single crystal exhibited no detectable decay during the data collection. Absorption corrections were applied using SADABS^[15]. The structure was solved by using the SHELXS-97^[16] program package and refined with the full-matrix least-squares technique based on F^2 using the SHELXTL-97^[17] program package. Hydrogen atoms on water molecules were located in a difference Fourier map and included in the subsequent refinement using restraints ($d(\text{O}-\text{H}) = 0.85 \text{ \AA}$, $d(\text{H}\cdots\text{H}) = 1.30 \text{ \AA}$) with $U_{\text{iso}}(\text{H}) = 1.5 U_{\text{eq}}(\text{O})$. Other hydrogen atoms were added theoretically and refined as riding atoms with a common fixed isotropic thermal parameter. Details about the crystal data are summarized in Tab. 1. Selected interatomic distances and bond angles are given in Tab. 2.

Tab. 1 Crystallographic data for the MOF

表 1 配合物的晶体数据

Empirical formula	$\text{C}_{120}\text{H}_{70}\text{N}_{20}\text{O}_{25}\text{Cd}_6$	Absorption coefficient/ mm^{-1}	1.161
Formula weight	2866.42	Crystal size/mm	$0.318 \times 0.249 \times 0.161$
Temperature / K	296(2)	Crystal color	colourless
Crystal system	Triclinic	$F(000)$	2836
Space group	$P\bar{1}$	Reflections collected	81494
$a \times b \times c / \text{\AA}$	$10.49 \times 23.16 \times 25.61$	Unique reflections (R_{int})	20462 (0.1294)
$\alpha \times \beta \times \gamma / ^\circ$	$106.7 \times 95.25 \times 99.78$	$\theta_{\text{min}}, \theta_{\text{max}} / ^\circ$	1.05, 25.00
$V / \text{\AA}^3$	5808.9(4)	$R_1, wR_2 [I > 2\sigma(I)]^a$	0.0998, 0.2607
Z	2	R_1, wR_2 (all data) ^a	0.1696, 0.3030
$D_c / \text{g}\cdot\text{cm}^{-3}$	1.639	Goodness-of-fit (on F^2)	1.097
		$\Delta\rho$ max, $\Delta\rho$ min ($\text{e}\cdot\text{\AA}^{-3}$)	4.419, -3.218

Tab. 2 Selected bond distances (\AA) and angles ($^\circ$) of the MOF

表 2 配合物的部分键长和键角

Bond	Bond dist/ \AA	Bond	Bond dist/ \AA	Bond	Bond dist/ \AA
Cd(1)-O(1)	2.183(9)	Cd(5)-O(3)	2.403(9)	Cd(4)-N(6)	2.225(10)
Cd(1)-N(5)	2.278(10)	Cd(5)-N(18)	2.450(11)	Cd(4)-N(8)#3	2.280(10)
Cd(1)-O(18)#1	2.348(9)	Cd(5)-O(21)#5	2.464(9)	Cd(4)-N(15)	2.354(13)
Cd(1)-N(10)	2.355(10)	Cd(6)-O(13)#6	2.151(12)	Cd(4)-N(16)	2.382(13)
Cd(1)-N(9)	2.449(10)	Cd(6)-O(21)#5	2.277(8)	Cd(4)-O(24)#3	2.445(10)
Cd(1)-O(18)	2.528(9)	Cd(6)-N(1)	2.297(9)	Cd(4)-O(15)	2.471(12)
Cd(2)-N(2)	2.277(10)	Cd(6)-N(20)	2.395(11)	Cd(5)-O(7)#4	2.159(11)
Cd(2)-N(3)	2.278(10)	Cd(6)-N(19)	2.399(11)	Cd(5)-N(7)#5	2.296(10)
Cd(2)-N(12)	2.366(10)	Cd(6)-O(3)	2.579(9)	N(8)-Cd(4)#7	2.280(10)
Cd(2)-N(11)	2.372(11)	C(13)-O(7)	1.182(18)	O(7)-Cd(5)#4	2.159(11)
Cd(2)-O(9)	2.403(11)	C(13)-O(8)	1.253(19)	O(13)-Cd(6)#8	2.151(12)
Cd(2)-O(6)	2.413(10)	C(22)-O(9)	1.201(17)	O(18)-Cd(1)#1	2.348(9)
Cd(3)-O(20)#2	2.163(16)	C(22)-O(10)	1.313(18)	O(20)-Cd(3)#2	2.163(16)
Cd(3)-O(19)	2.230(13)	C(34)-O(15)	1.209(18)	O(21)-Cd(6)#5	2.277(8)
Cd(3)-N(4)	2.307(11)	C(34)-O(16)	1.332(19)	O(21)-Cd(5)#5	2.464(9)
Cd(3)-N(13)	2.335(14)	C(48)-O(24)	1.245(15)	O(24)-Cd(4)#7	2.445(10)

Cd(3)-O(12)	2.368(12)	C(48)-O(23)	1.294(16)		
Cd(3)-N(14)	2.422(13)	N(7)-Cd(5)#5	2.296(10)		
Angle	(°)	Angle	(°)	Angle	(°)
O(1)-Cd(1)-N(5)	104.0(3)	N(6)-Cd(4)-N(8)#3	140.7(4)	O(9)-Cd(2)-O(6)	116.1(3)
O(1)-Cd(1)-O(18)#1	91.8(3)	N(6)-Cd(4)-N(15)	118.7(4)	O(20)#2-Cd(3)-O(19)	118.1(5)
N(5)-Cd(1)-O(18)#1	132.8(3)	N(8)#3-Cd(4)-N(15)	94.8(4)	O(20)#2-Cd(3)-N(4)	144.7(5)
N(5)-Cd(1)-N(10)	104.6(3)	N(8)#3-Cd(4)-N(16)	98.8(4)	O(19)-Cd(3)-N(4)	84.6(4)
O(18)#1-Cd(1)-N(10)	87.6(3)	N(15)-Cd(4)-N(16)	71.0(5)	O(20)#2-Cd(3)-N(13)	93.5(5)
O(1)-Cd(1)-N(9)	81.8(3)	N(6)-Cd(4)-O(24)#3	88.1(4)	O(20)#2-Cd(3)-O(12)	77.9(5)
N(5)-Cd(1)-N(9)	97.6(3)	N(8)#3-Cd(4)-O(24)#3	71.4(3)	O(19)-Cd(3)-O(12)	98.7(4)
O(18)#1-Cd(1)-N(9)	128.8(3)	N(15)-Cd(4)-O(24)#3	145.9(4)	N(4)-Cd(3)-O(12)	71.7(4)
N(10)-Cd(1)-N(9)	68.9(4)	N(16)-Cd(4)-O(24)#3	80.3(4)	N(13)-Cd(3)-O(12)	168.2(5)
N(5)-Cd(1)-O(18)	70.4(3)	N(8)#3-Cd(4)-O(15)	94.8(4)	O(19)-Cd(3)-N(14)	148.5(5)
O(18)#1-Cd(1)-O(18)	64.4(3)	N(15)-Cd(4)-O(15)	84.6(4)	O(12)-Cd(3)-N(14)	101.9(4)
N(9)-Cd(1)-O(18)	151.7(3)	O(24)#3-Cd(4)-O(15)	126.5(4)	N(18)-Cd(5)-O(21)#5	161.4(3)
N(2)-Cd(2)-N(3)	139.9(3)	O(7)#4-Cd(5)-N(7)#5	117.2(4)	O(13)#6-Cd(6)-O(21)#5	105.2(4)
N(2)-Cd(2)-N(12)	117.4(4)	O(7)#4-Cd(5)-N(17)	137.6(4)	O(13)#6-Cd(6)-N(1)	99.6(4)
N(3)-Cd(2)-N(12)	92.8(4)	N(7)#5-Cd(5)-N(17)	102.1(4)	O(21)#5-Cd(6)-N(1)	131.2(3)
N(2)-Cd(2)-N(11)	97.6(4)	O(7)#4-Cd(5)-O(3)	83.3(4)	O(13)#6-Cd(6)-N(20)	151.1(4)
N(3)-Cd(2)-O(9)	72.9(4)	N(7)#5-Cd(5)-N(18)	113.3(3)	O(13)#6-Cd(6)-N(19)	83.1(4)
N(12)-Cd(2)-O(9)	88.8(4)	N(17)-Cd(5)-N(18)	69.2(4)	O(21)#5-Cd(6)-N(19)	117.7(4)
N(2)-Cd(2)-O(6)	71.9(3)	O(7)#4-Cd(5)-O(21)#5	115.1(3)	N(1)-Cd(6)-N(19)	106.4(3)
N(3)-Cd(2)-O(6)	92.0(4)	N(7)#5-Cd(5)-O(21)#5	69.6(3)	N(20)-Cd(6)-N(19)	68.3(4)
N(12)-Cd(2)-O(6)	155.0(4)	N(17)-Cd(5)-O(21)#5	92.2(3)	O(21)#5-Cd(6)-O(3)	63.3(3)
N(11)-Cd(2)-O(6)	85.6(4)	O(3)-Cd(5)-O(21)#5	63.5(3)	N(19)-Cd(6)-O(3)	156.4(4)

Symm. code: #1 -x+2,-y+2,-z+1; #2 -x+1,-y+2,-z; #3 x+1,y,z+1; #4 -x+1,-y+1,-z; #5 -x,-y+1,-z; #6 x-1,y,z; #7 x-1,y,z-1; #8 x+1,y,z.

2.2 Data collection and structure analysis

Single-crystal analysis showed that this MOF is crystallized in the triclinic space group $P\bar{1}$, and the asymmetric unit cell contains six inequivalent crystallography Cd^{2+} ions, one μ_4 -CPhIDC⁴⁻ ion, one μ_3 -HCPPhIDC³⁻ ion, one μ_5 -HCPPhIDC³⁻, one μ_3 -H₂CPhIDC²⁻, six 1,10-phenanthroline molecules and one lattice water molecule.

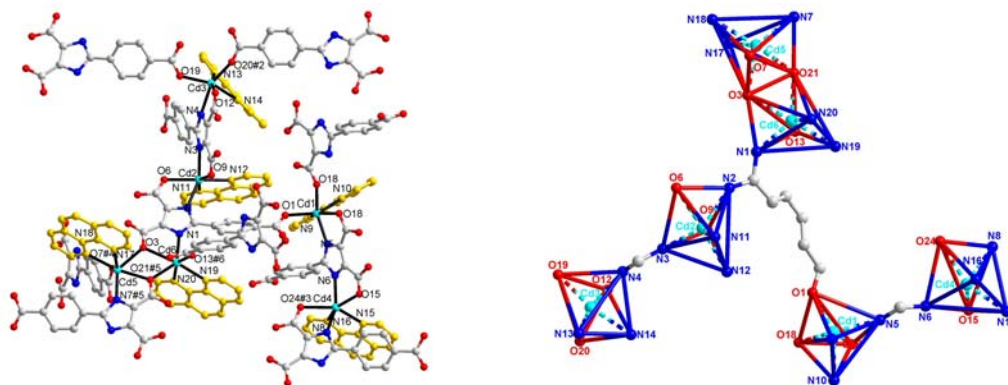


Fig. 1 (a) Ball-and-stick structural view of MOF; (b) View of the environment of Cd(II) ions for MOF

图 1 (a) 配合物的球棍分子结构图; (b) 配合物的六核配位环境

As is shown in Fig. 1a, each Cd^{2+} ion adopts a six-coordinated mode with distorted octahedral geometry. Each phen molecule with a crystallographic 2-fold axis bis-chelates one Cd^{2+} ion through two nitrogen atoms. The different coordination mode is as follows: Cd(1), Cd(3), Cd(5), Cd(6) are each coordinated by three nitrogen atoms (one from the imidazole carboxylic acid ligand, the others from one phen) and three oxygen atoms (from three imidazole carboxylic acid ligands) to form four $[\text{CdN}_3\text{O}_3]$ units. Whereas, Cd(2) and Cd(4) are both six-coordinated by two nitrogen atoms (from two imidazole carboxylic acid ligands), two nitrogen atoms (from one phen) and two oxygen atoms (from two imidazole carboxylic acid ligands) to form two $[\text{CdN}_4\text{O}_2]$ units. In the $[\text{CdN}_3\text{O}_3]$ unit, the imidazole carboxylic acid ligand with a crystallographic 2-fold axis

through N, O bis-chelating and a single axis through O mono-chelating in a $\mu_3\text{-}\kappa\text{O}:\kappa^2\text{O}'$, $\text{N}:\kappa\text{O}''$ coordination fashion. In $[\text{CdN}_4\text{O}_2]$ cell, each imidazole carboxylic acid ligand is coordinated with Cd^{2+} ion through N, O atoms by bis-chelate mode. In addition, the coordination modes of the three forms are different (Scheme 1 a, b, and c), and so the function of the 3D-supramolecular structure is. The Cd-O distances, the Cd-N distances and bond angles (shown in Tab. 1) for this MOF are in the normal regions which are comparable to values reported in literatures^[18].

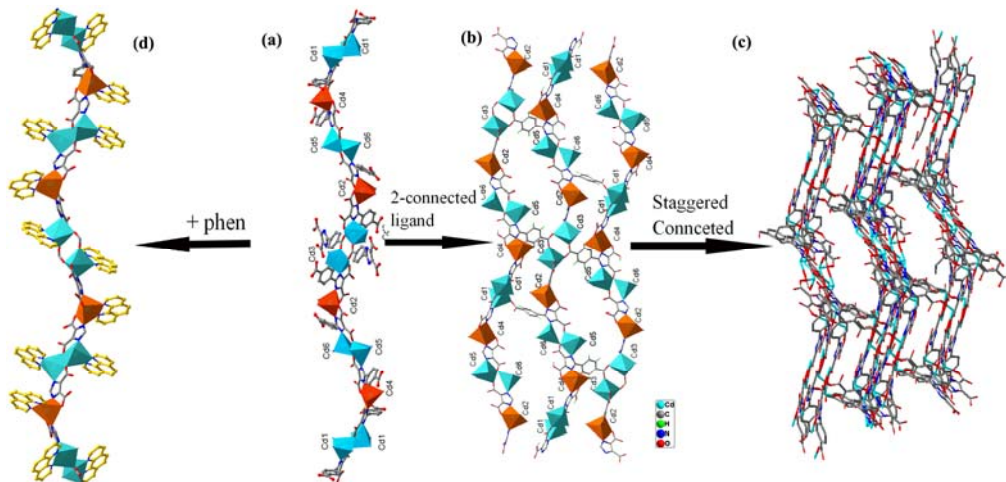


Fig. 2 (a) The 1D chain structure without phen for MOF; (b) The 2D structure without phen for MOF; (c) 3D supramolecular framework without phen for MOF; (d) 1D chain structure with phen for MOF

图 2 (a) 配合物的一维链状结构; (b) 配合物的二维网络结构; (c) 配合物的三维空间结构; (d) 补充邻菲咯啉辅助配体的一维链状结构

Adjacent Cd ions are bridged by two oxygen atoms from two imidazole carboxylic acid ligands to form a 1D chain structure (Fig. 2a) with the staggered different coordination mode reside at the sides of it. The pillaring functions of the ligand connected to two adjacent 1D chains to expand the 1D chain into 2D network (Fig. 2b), in which the imidazole carboxylic acid ligand can be simplified to a 2-connected linker. The staggered 2D network connected with 28-membered, 40-membered and 44-membered rings and thus show a rugged terrain shape bridged by the adjacent 2D network and then finally expand to “S” size 3D supramolecular framework^[19] (Fig. 2c). In addition, the phen molecule contributes to stabilizing the crystal structure with the function of $\pi \cdots \pi$ accumulation (Fig. 2d).

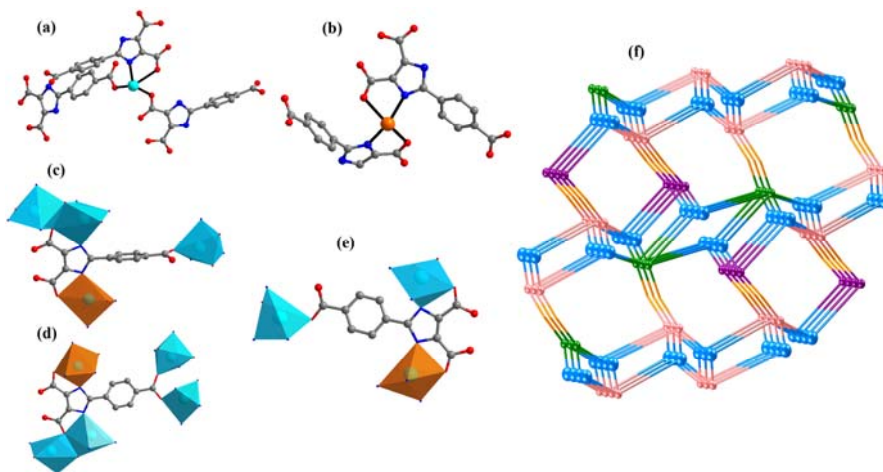


Fig. 3 (a) $\text{Cd}(1)$ ($\text{Cd}(3)$, $\text{Cd}(5)$, $\text{Cd}(6)$) 3-connected coordinated with three imidazole carboxylic acid ligands; (b) $\text{Cd}(4)$ ($\text{Cd}(2)$) 2-connected coordinated with two imidazole carboxylic acid ligands; (c) HCPHIDC^{3-} (pink) 4-connected coordinated with three $\text{Cd}(1)$ ions (blue) and one $\text{Cd}(4)$ ion (orange); (d) $\text{H}_2\text{CPhIDC}^{2-}$ (green) 5-connected coordinated with four $\text{Cd}(1)$ ions (blue) and one $\text{Cd}(4)$ ion (orange); (e) $\text{H}_2\text{CPhIDC}^{2-}$ (purple) 3-connected coordinated with two $\text{Cd}(1)$ ions and one $\text{Cd}(4)$ ion; (f) The (3,3,4,5)-topological connected for MOF

图 3 (a) 以 $\text{Cd}(1)$ ($\text{Cd}(3)$, $\text{Cd}(5)$, $\text{Cd}(6)$) 为节点连接了三个咪唑羧酸配体的 3 连接点; (b) 以 $\text{Cd}(4)$ ($\text{Cd}(2)$) 为节点连接了两个咪唑羧酸配体的 2 节点; (c) 以 HCPHIDC^{3-} (粉色) 为节点连接了四个 Cd 离子 (三个 $\text{Cd}(1)$ 离子和一个 $\text{Cd}(4)$ 离子) 的 4 节点; (d) 以 $\text{H}_2\text{CPhIDC}^{2-}$ (绿色) 为节点连接了五个 Cd 离子 (四个 $\text{Cd}(1)$ 离子和一个 $\text{Cd}(4)$ 离子) 的 5 节点; (e) 以 $\text{H}_2\text{CPhIDC}^{2-}$ (紫色) 为节点连接了三个 Cd 离子 (两个 $\text{Cd}(1)$ 和一个 $\text{Cd}(4)$); (f) 配合物的 (3,3,4,5)-连接的拓扑结构

From the topological point of view, each Cd ion (Cd(1), Cd(3), Cd(5), Cd(6)) linked to three imidazole carboxylic acid ligands represents a 3-connected node (Fig. 3a), each Cd(4) (or Cd(2)) ion linked to two imidazole carboxylic ligands represents a bond (Fig. 3b), each HCPHIDC³⁻ ion linked to three Cd(1) ions and one Cd(4) ion represents a 4-connected node (Fig. 3c), each HCPHIDC³⁻ ion linked to four Cd(1) ions and one Cd(2) ion represents a 5-connected node (Fig. 3d), each H₂CPhIDC²⁻ ligand serves as a 3-connected node by combining two Cd(1) ions and one Cd(4) ion (Fig. 3e). Thus the 3D network can be regarded as a pentanodal (3,3,4,5)-connected with the Schläfli symbol of $(4 \cdot 8 \cdot 10)^2(4 \cdot 8^2)(8^3)(4^2 \cdot 8^4 \cdot 10^4)(4 \cdot 8^3 \cdot 10^2)$ as shown in (Fig. 3f). To date, there is no example of (3,3,4,5)-connected MOFs are reported and thus present a new tetra-nodal (3,3,4,5)-connected 3D framework topology.

2.3 Photoluminescent property

As illustrated in Fig. 4, the solid-state photoluminescence spectra at room temperature for the H₄CPhIDC ligand and MOF are observed to have their main emission at 524 nm and 527 nm ($\lambda_{\text{ex}}=467$ nm), respectively. The imidazole ligand and the MOF can both emit certain intensity green luminescence. The green luminescence in the MOF comes from the H₄CPhIDC ligand and litter smaller than it. The bathochromic shift effect for the MOF may be ascribed to the decreased electron density after coordination, and thus the energy level spacing ($\pi^*-\pi$) is lower.

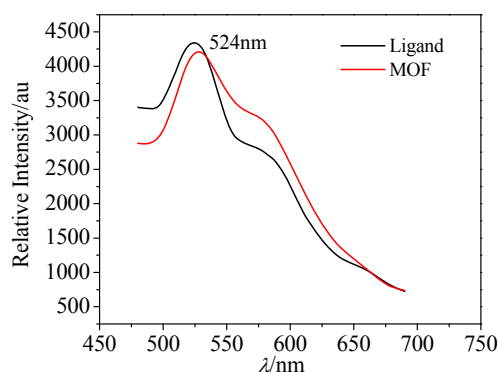


Fig. 4 Fluorescence spectra for ligand and MOF

图 4 配体和配合物的荧光光谱图

2.4 EB-DNA binding study by fluorescence spectra

The interaction of the H₄CPhIDC ligand and MOF with calf thymus DNA (ct-DNA) was studied by an EB fluorescent probe. The experiment was carried out by adding different volumes of compound solution (10^{-4} mol/L for H₄CPhIDC ligand or the MOF) to a 10 mL colorimetric cylinder and then prepared 2 h in advance, which contained 2.0 mL 100 $\mu\text{g/mL}$ EB, 1.0 mL 200 $\mu\text{g/mL}$ ct-DNA, and 2.0 mL tris-HCl buffer solution (pH 7.4), then the mixed solution were diluted with double-distilled water. The final solutions were incubated for 12 h at 4 $^{\circ}\text{C}$. The fluorescence was recorded at an excitation wavelength of 251 nm and emission wavelength between 520 nm and 700 nm.

Fig. 5 shows that the emission spectra of EB bounded to DNA with the H₄CPhIDC ligand and with or without the MOF. As increasing the concentration of the ligand and MOF, the emission intensity at 592 nm of EB-DNA system decreased in different degrees.

According to the classical Stern-Volmer equation^[20]: $I_0/I = 1 + K_{\text{sq}} r$, where I_0 and I represents the fluorescence intensities in the absence or presence of the compounds, respectively. r is the concentration ratio of the compounds to DNA. K_{sq} is a linear Stern-Volmer quenching constant. The K_{sq} value is obtained as the slope of I_0/I versus r linear plot.

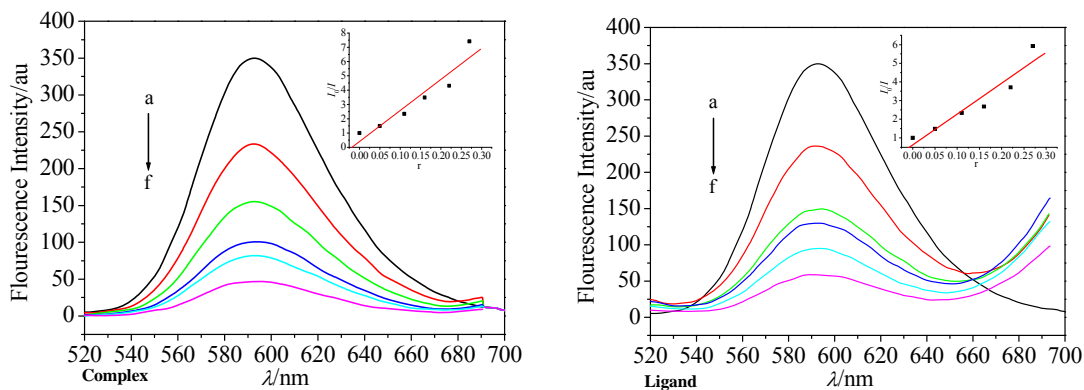


Fig. 5 Emission spectra of EB-DNA system in the absence and presence of the H₄CPhIDC ligand, MOF from a to f: $r = [\text{Compound}]/[\text{DNA}] = 0, 0.05, 0.11, 0.16, 0.22, 0.27$

图 5 配体以及配合物与 EB-DNA 相互作用荧光猝灭曲线图

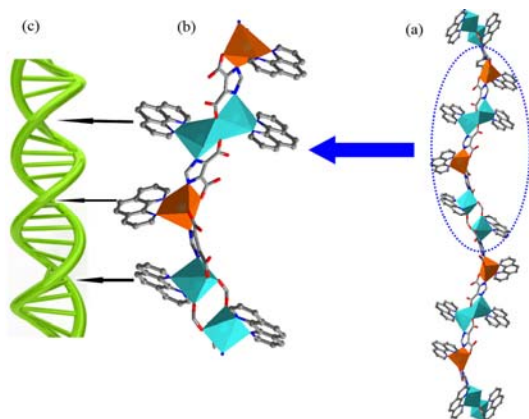


Fig. 6 (a) 1D chain for MOF; (b) 1D chain for MOF binding DNA with phen planar molecules; (c) DNA double helices

图 6 (a) 配合物的一维链状结构; (b) 一维链状配合物中的邻菲咯啉分子与 DNA 相互作用的模拟图; (c) DNA 双螺旋结构

From the inset in Fig. 5, the K_{sq} value were 16.53 and 22.77 for imidazole carboxylic acid ligand and MOF. It suggested that the interaction of the ligand itself with DNA were strong and could release some free EB from EB-DNA, because of the presence of benzene and imidazole rings. For the MOF, it has stronger interaction with the DNA (related to the H₄CPhIDC ligand) because of adding the big phen planar molecules and could release more free EB form EB-DNA, which could be ascribed to the fact that compounds had already been inserted into the DNA structure (Fig. 6).

2.5 BSA interaction experiments

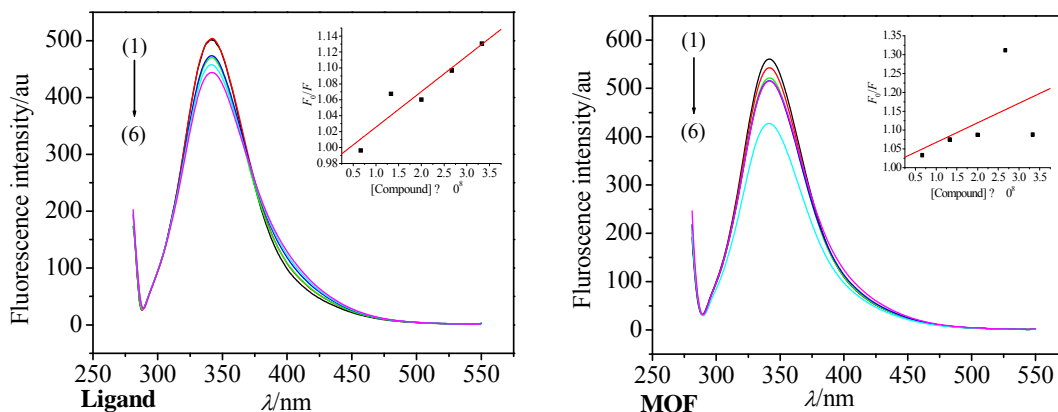


Fig. 7 Synchronous fluorescence spectra of BSA in the absence and presence of the H₄CPhIDC ligand or MOF. [BSA] = 4.98×10^{-7} mol/L; [compound] $\times 10^8 = 0, 0.667, 1.33, 2.00, 2.67$ and 3.33 mol/L, from (1) to (6), respectively

图 7 配体与配合物与 BSA 相互作用的荧光光谱图

The H₄CPhIDC ligand or MOF (1.0×10^{-5} mol/L) were added to a solution containing 1.0 mL 4.98×10^{-7} mol/L BSA and 2.0 mL Tri-HCl buffer. Fluorescence spectra were obtained by recording the emission spectra (255~500 nm) corresponding to the excitation wavelength at 255 nm. The H₄CPhIDC ligand and MOF quenching the BSA fluorescence give similar results as DNA binding experiment. As is shown in Fig. 7, both H₄CPhIDC and MOF can quench the fluorescence of BSA. The results showed that the intensity of the fluorescence peak of BSA decreased with increasing concentrations of the H₄CPhIDC ligand and MOF at 345nm, which implied that MOF has stronger interaction with BSA than H₄CPhIDC.

In order to verify the quenching mechanism, the fluorescence quenching was assumed to be dynamic quenching. The quenching rate constants can be determined by the Stern-Volmer equation^[21]: $F_0/F = 1 + K_q \tau_0 [Q]$, where F_0 and F are the fluorescence intensities of BSA in the absence and presence of the compounds, respectively. $[Q]$ is the concentration of the compounds. For many proteins, τ_0 (the lifetime of the fluorophore) is known to be approximately 10^{-8} s^[22]. The calculated quenching rate constants K_q were 3.3×10^{11} L·mol⁻¹·s⁻¹ to 3.1×10^{12} L·mol⁻¹·s⁻¹. These value were greater than the maximum possible value for diffusion-limited quenching in water (2×10^{10} L·mol⁻¹·s⁻¹), which suggested that the quenching mechanism of H₄CPhIDC (MOF) to BSA was static quenching from the formation of a ground-state complex between the fluorophore and quencher^[23].

3 Conclusions

In summary, a new H₃IDC derivative 2-(4'-carboxyphenyl)-1*H*-imidazole-4,5-dicarboxylic acid (H₄CPhIDC) was purposely synthesized by condensation and oxidation reactions based on *o*-phenylenediamine and methyl 4-formylbenzoate. It is worthwhile to note that it's the first time to introduce carboxyl-containing group on the 2-position of H₃IDC and successfully applied to constructing [Cd₆(CPhIDC)(HCPHIDC)₂(H₂CPhIDC)(phen)₆]·H₂O MOF. The MOF is a six-core "S" size 3D supramolecular framework with (3,3,4,5)-connected $(4 \cdot 8 \cdot 10)^2(4 \cdot 8^2)^2(8^3)$ $(4^2 \cdot 8^4 \cdot 10^4)(4 \cdot 8^3 \cdot 10^2)$ topology. Moreover, the luminescent property showed that the imidazole ligand and MOF can both emit certain intensity green luminescence. The interaction of the ligand and MOF with DNA was strong and could release some free EB from EB-DNA, because of the present of benzene and imidazole rings. The MOF has stronger interaction with DNA (related to the H₄CPhIDC ligand) because of adding the big phen planar molecules and could release more free EB form EB-DNA, which could be ascribed to the fact that compounds had been inserted into the DNA structure. In addition, the quenching mechanism of H₄CPhIDC (MOF) to BSA was static quenching from the formation of a ground-state compound between the fluorophore and quencher. This class of materials may provide a new impetus to the construction of novel biological activities MOF materials.

References

- [1] A M Voutchkova, L N Appelhans, A R Chianese et al. *J. Am. Chem. Soc.*, 2005, 127(50): 17624 ~ 17625.
- [2] L Yi, X Yang, T B Lu et al. *Cryst. Growth Des.*, 2005, 5(3): 1215 ~ 1219.
- [3] Y H Luo, Y H Yu, J J Yang et al. *CrystEngComm.*, 2014, 16: 47 ~ 50.
- [4] (a) C Huang, J Wu, D M Chen et al. *Chinese J. Inorg. Chem.*, 2015, 1(31): 109 ~ 113; (b) H Chen, J Y Xie, J Y Si. *Chem. Res. Appl.*, 2005, 17(6): 799 ~ 801.
- [5] B Panella, M Hirscher, H Pütter et al. *Adv. Funct. Mater.*, 2006, 16(4): 520 ~ 524.
- [6] N Stock, S Biswas. *Chem. Rev.*, 2012, 112(2): 933 ~ 969.
- [7] B Arstad, H Fjellvåg, K O Kongshaug et al. *Adsorption*, 2008, 14(6): 755 ~ 762.
- [8] C Janiak, J K Vieth. *New J. Chem.*, 2010, 34(11): 2366 ~ 2388.
- [9] S K Henninger, S K Habib, C Janiak. *J. Am. Chem. Soc.*, 2009, 131(8): 2776 ~ 2777.
- [10] A Torrisi, G B Bell, C Mellot-Draznieks. *Cryst. Growth Des.*, 2010, 10(7): 2839 ~ 2841.
- [11] K Li, D H Olson, J Y Lee et al. *Adv. Funct. Mater.*, 2008, 18(15): 2205 ~ 2214.
- [12] C Y Lee, O K Farha, B J Hong et al. *J. Am. Chem. Soc.*, 2011, 133(40): 15858 ~ 15861.
- [13] (a) H Sharghi, O Asemiani, R Khalifeh. *Synth. Commun.*, 2008, 38(7): 1128 ~ 1136; (b) C Tan, Q Wang. *Inorg. Chem.*, 2011, 50(7): 2953 ~ 2956.
- [14] (a) A Ghosh, K Prabhakara Rao, R A Sanguramath et al. *J. Mol. Struct.*, 2009, 927(1 ~ 3): 37 ~ 42; (b) F Dang, X Wang, X Han et al. *Monatsh Chem.*, 2009, 140(6): 615 ~ 617; (c) W Wang, X Niu, Y Ga, et al. *Cryst. Growth Des.*, 2010, 10(9): 4050 ~ 4059.
- [15] G M Sheldrick, SADABS: Program for Empirical Absorption Correction of Area Detector Data, University of Göttingen, Germany 1997.
- [16] G M Sheldrick, SHELXS 97, Program for crystal structure solution, University of Göttingen, Germany 1997.

- [17] G M Sheldrick, SHELXL 97, Program for crystal structure refinement, University of Göttingen, Germany 1997.
- [18] W Lin, L Ma, O R Evans. Chem. Commun., 2000, (22): 2263 ~ 2264.
- [19] X Jing, T Zhao, B Zheng et al. Inorg. Chem. Commun., 2011, 14(1): 22 ~ 25.
- [20] J R Lakowicz, G Weber. Biochemistry, 1973, 12(21): 4161 ~ 4170.
- [21] Q Guo, L Li, J Dong et al. Spectrochim. Acta A, 2013, 106: 155 ~ 162.
- [22] X W Li, Y T Li, Z Y Wu et al. Inorg. Chim. Acta, 2012, 390: 190 ~ 198.
- [23] N M Urquiza, L G Naso, S G Manca et al. Polyhedron, 2012, 31(1): 530 ~ 538.